



## Geometrical Analysis of the Asos and Dokan Anticlines in Imbricated and High Folded Zones of the Zagros Fold-Thrust Belt, Iraqi Kurdistan Region

Soran H Syan, Abdulla Amir Omar

*Department of Earth Sciences and Petroleum, College of Science, Salahaddin University, Erbil, Iraq*

Received: 25 Aug. 2024 Received in revised form: 2 Sep. 2024 Accepted: 10 Sep. 2024

Final Proofreading: 27 Sep. 2024 Available online: 25 Feb. 2025

### ABSTRACT

The Asos and Dokan anticlines are situated in the Imbricated and High Folded zones, respectively, in the NW segment of Zagros Fold and Thrust Belt within the Kurdistan Region of Iraq. The balanced section across these structures was constructed manually on the graph-paper by employing the kink-band methods and restored to their pre-deformed shape, the constructed balanced cross-section was constrained by integrating intensive surface geological observations and available subsurface seismic sections. The study aims to understanding the geometry of the structures as well as fold and fault architecture at depth. The structures are slightly asymmetrical with steeper forelimb and wide crestal region. The average horizontal shortening values of the Dokan and Asos anticlines are (7.21 %) and (17.05 %) respectively, and the fault-related shortening decrease upsection. The Asos anticline exhibits greater fault-related shortening values compared to the Dokan structure due to higher deformation intensity via thrusting processes. The studied section implies that the structures representing thrust-related anticline and the Dokan anticline show pop-up geometry, while Asos exhibits imbricate fan thrust.

**Keywords:** Asos and Dokan anticlines, Balanced cross-section, Shortening, Structural style, Kink method.

**Name:** Soran H Syan **E-mail:** [soran.syan@su.edu.krd](mailto:soran.syan@su.edu.krd)



©2025 THIS IS AN OPEN ACCESS ARTICLE UNDER THE CC BY LICENSE  
<http://creativecommons.org/licenses/by/4.0/>

## التحليل الهندسي لطبتي أسوس ودوكان ضمن منطقتي التراكيب الزاحفة والطيات العالية من حزام

طي - زحف زاكروس، إقليم كردستان العراق

سوران حسن سيان، عبد الله عامر عمر

قسم علوم الأرض والنفط، كلية العلوم، جامعة صلاح الدين، أربيل، العراق

### الملخص

تم دراسة تركيبية طبتي أسوس ودوكان في منطقتي التراكيب الزاحفة والطيات العالية على التوالي في الجزء الشمالي الغربي من حزام طي - زحف زاكروس في إقليم كردستان العراق. تم إنشاء المقطع العرضي المتوازن والمعاد تشكيله يدويا باستخدام طريقة كوك عبر هذين التركيبين من خلال دمج الملاحظات الجيولوجية الحقلية المكثفة والمقاطع الزلزالية تحت السطحية المتاحة. تهدف الدراسة إلى فهم هندسة التراكيب وهيكلية الطيات والصدوع ووصف التقدم التتابعي للطيات المحدبة. تكون التراكيب غير متناظرة إلى غير متناظرة قليلاً مع جناح أمامي أكثر ميلاً ومناطق قمية واسعة. يبلغ معدل قيم التقصير الأفقي لطبتي دوكان وأسوس إلى (7.21 %) و(17.05 %) على التوالي، يتناقص التقصير المتعلق بالصدوع باتجاه الطبقات العلوية. وتظهر طية أسوس قيم تقصير متعلقة بالصدوع أكبر مقارنةً بطية دوكان بسبب شدة التشويه الأعلى عبر عمليات الزحف. يشير المقطع المدروس إلى أن التراكيب تمثل طيات محدبة متعلقة بالزحف، وتظهر طية دوكان بنية بروزية، بينما تظهر طية أسوس صدوع زاحفة مروحية متراكبة الشكل.

### 1. INTRODUCTION

Throughout geological history, Fold-Thrust belts have formed as the primary way the crust accommodated shortening<sup>(1)</sup>. Since the seminal work describing the kinematics and geometry of thrust-related folding<sup>(2)</sup>. The Zagros Fold-Thrust Belt (ZFTB) as a richest province of oil and gas become.

Despite the excellent surface exposure of the Zagros anticlinal folds in the Zagros Suture, Imbricate and High Folded zones, their reconstruction at depth is still the matter of their investigation and precise interpretation. These include (i) lack or restricted availability of seismic sections; (ii) safety (landmines and unexploded ordnance) (iii) rugged terrain and complexity of the structures (iv) nature and thickness of folded uppermost sedimentary cover, and (v) the existence of multiple detachment levels.

The main objective of this study is to (1) investigate about the fold and fault shape at surface and with depth, (2) understanding the geometrical

properties, and (3) determine the shortening percentage through comparing the balanced and retrodeformed cross-sections.

The area of study is located (~55 km) east of the Erbil city and (~60 km) northwest of northwest of Sulaimani city, Kurdistan Region of Iraq (KRI). It is bounded by longitudes (44° 31' 17") and (45° 16' 54" E) and latitudes (35° 48' 15") and (36° 28' 05" N), and covering (~2332 km<sup>2</sup>) in the Iraqi Kurdistan Region (Fig.1). The studied region consists of two anticlinal structures named the Asos and Dokan anticlines with Raniya and Taqaltu synclines. Tectonically, Asos anticline is located within the Imbricated Zone (IZ), while the Dokan is located within the High Folded Zone (HFZ) (Fig.1).

### 2. GEOLOGICAL SETTING

#### 2.1. Tectonic setting

The NW segment of the NW-SE trending Zagros Orogenic Belt is part of the Alpine-Himalayan Mountain series that comprises the study area in

KRI. The Neogene Period witnessed a persistent collision between continental plates along the Zagros belt, resulting in a significant increase in the amount of shortening across the ZFTB that led to the formation of the Zagros foreland<sup>(3)</sup>.

The Zagros belt is bounded by the Main Zagros Thrust Fault (MZTF) and the Main Recent Fault to the NE, together forming the Suture Zone of this belt. In the SW, the Mountain front flexure and High Zagros Fault are the two main structures of the Zagros belt<sup>(4)</sup>. During contractional tectonic processes, the Phanerozoic sedimentary succession underwent thrusting, folding and strike-slip faulting activities over the Precambrian basement.

The NW-SE oriented ZFTB in KRI can be divided into five distinct tectonic zones depending on deformation intensity, morphotectonic characteristics, mechanical stratigraphy, and structural style. The subdivisions from foreland toward hinterland are: (1) Mesopotamian Foreland Basin (MFB), (2), Low Folded Zone (LFZ) or Foothill Zone (FHZ) (3) High Folded Zone (HFZ), (4) Imbricated Zone (IZ), and (5) the Zagros Suture Zone (ZSZ) (Fig. 1). The boundary between the HFZ and the FHZ is defined by the Mountain Front Flexure (MFF) and coincides with a deep-seated fault along the SW- limb of the Kosrat and Dokan anticline<sup>(3)</sup>.

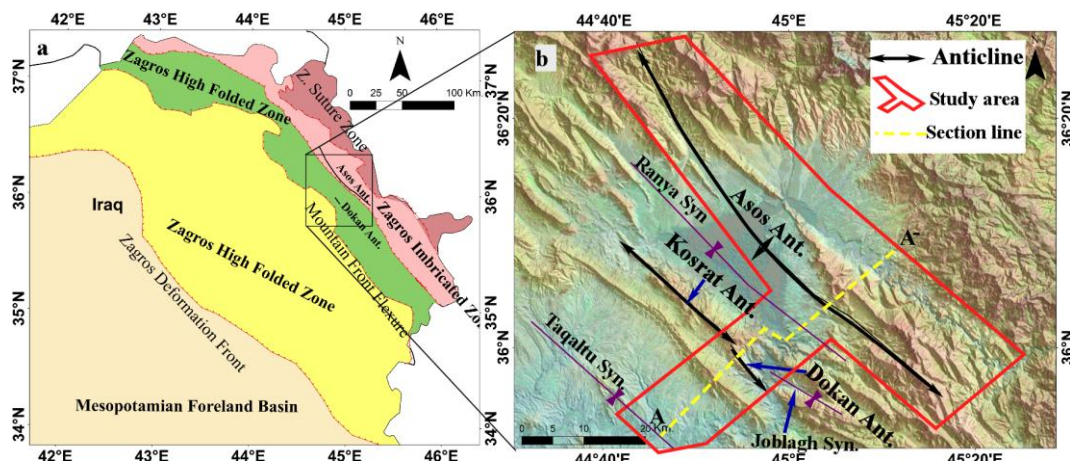


Fig. 1: a) Tectonic zones of northern Iraq as a portion of the ZFTB (modified after<sup>(3), (5), (6), (7)</sup>). b) enlarged map shows the studied anticlines.

## 2.2. Stratigraphy of the study region

The exposed successions represented by 19 formations that deposited during Late Triassic (Baluti Formation) to Recent deposits (Fig. 3). The Mesozoic to Cenozoic strata is primarily dominated by platform carbonates, with local occurrence of shales and evaporites<sup>(3)</sup>. The Paleogene unit comprises different mechanically weak and stiff formations with significantly different mechanical behavior and thickness. A more rigid carbonate unit (Palaeogene Khurmala-Sinjar, Avana and Pilia Spi Formations) form a

prominent and an easily recognized Haibat Sultan Mountain (HSM) ridge at the southwestern limb of Kosrat and Dokan anticlines, while the incompetent Paleogene units occupied the eroded area of this anticline (Fig. 2). The Neogene succession is deposited at SW limb of Dokan anticline and mainly composed of clastic rock and characterized by upward coarsening and thickening packages. The Dokan Conglomerate is a lithostratigraphic unit of Pliocene-Pleistocene age recognize by that resemblance to Neogene formations<sup>(8)</sup>.

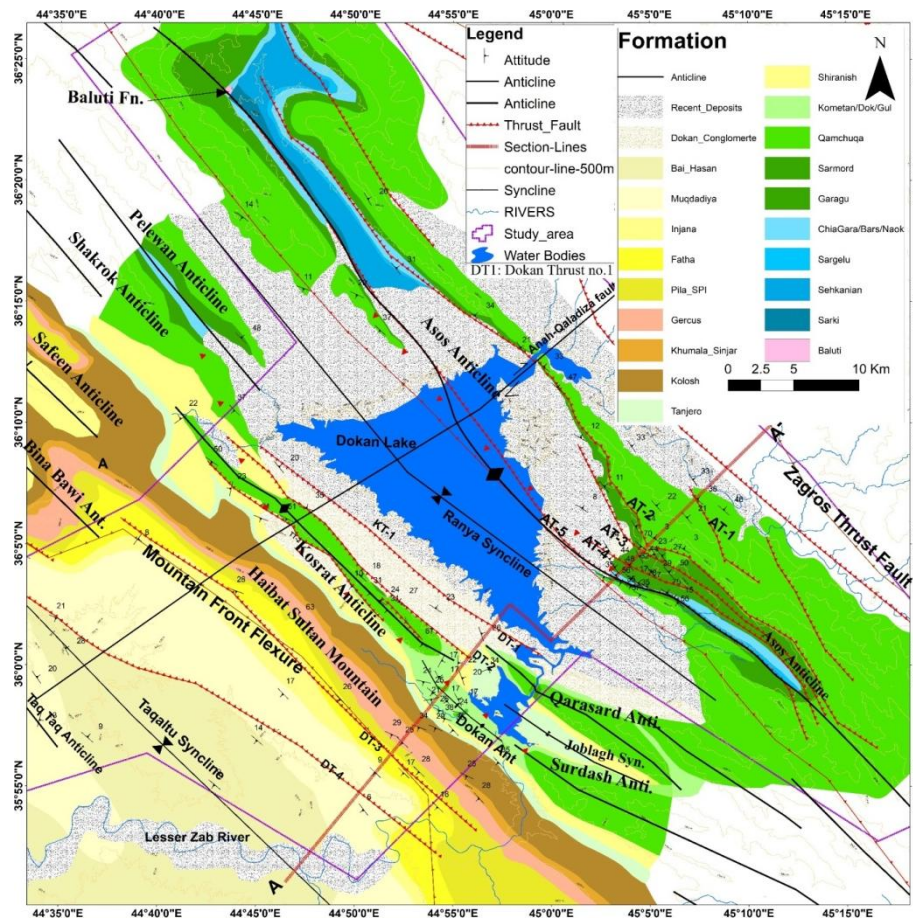


Fig. 2: Comprehensive geologic map of the Asos and Dokan anticlines including nearby structures and MZF.

### 3. METHODOLOGY

In conducting this structural study, the field observation data were integrated with available subsurface data (well and seismic section) to draw balanced and restored cross-section and geometrical analysis. Therefore, more than 42 field stations (235 bedding orientation) were measured from observable surface geological features along the best representative section path across the fold hinge line. Field measurements along a cross-section A-A<sup>-</sup> were plotted on a comprehensive topographic base map at a scale of (1:20,000), which was also used for constructing geological map and sections. Length of section A-A<sup>-</sup> is (~ 45.9 km) across Asos and Dokan anticlines that investigated through 42 field stations (Fig. 2). The balanced section was constructed manually on the graph-paper by employing the kink-band methods and restored to its pre-deformed shape<sup>(9, 10)</sup>.

The balanced sections were manually restored to their un-deformed state by removing the entire cumulative effects of folding and faulting processes. Then the section digitized using Canvas software v14.

### 4. RESULTS: STRUCTURAL ANALYSES

For giving detail structural properties of the Asos and Dokan anticlines, the explanation can be done under three categories in (i) Map view, (ii) cross-sectional description and (iii) Geometric Analysis.

#### 4.1. Map view description of Asos and Dokan structures

A comprehensive geological map has constructed for Asos, Kosrat and Dokan thrust anticlines including their surrounding areas (Fig. 2).

The Asos is a major fold structure with NW-SE oriented and double plunging fold axis, which is located near the NE margin of the Arabian plate and covers a part imbricated zone of ZFTB. The Asos anticline is traceable for about 91km along its

length, and is about (8 – 10 km) in width, with crestal line elevation of (~ 2534 m). The structure was raised at both plunge areas but lowered in the middle to about (500 m). (Fig. 2). The Pelewan, Kosrat and Qara Sard anticlines determined the W and SW of the structure and separated by Ranya syncline, while the MZF occupy in the NE side. The outcropped stratigraphic succession spans from the Late Triassic (Baluti Formation) to the late Cretaceous Bekhme/Kometan and Gulnery Formations (Fig. 3).

The backlimb (NE limb) of the structure is broader and covers majority of the area and has a nearly straight outline shape but shows arcuate with hinterlandward convex shape in the middle of the structure. In contrast, the hinge line is arcuate with the forlandward convex shape. This main swing in axial trend and outline coincides with the cross-cutting off this structure with Anah- Qalat Dizeh (Qaladza) transversal fault (AQF). The AQF is the most impressive transversal fault both tectonically and morphologically and separates some anticline and passes along Lesser Zab<sup>(3, 11)</sup>. As a result of this fault, Asos Anticline divide into two segments, the northwestern segment located near to Ranya city while the southeastern segment situated in Bingrd district (Fig. 2). Some authors (e.g., <sup>(12, 13)</sup>) considered its northern segment as Ranya anticline that plunged near Ranya city, but the field work observations revealed both segments are a single structure and it divided by the Anah-Qalat-Dizeh transversal fault.

The effect of five NW-SE trending main thrusts intensively disturbed the Asos thrustfold (Fig. 2 and Fig.3). These SW- verging listric forethrusts named from the NE toward SW and abbreviated to

AT1, AT2, AT3, AT4, and AT5 which exhibits either slightly sigmoidal or gently bowed fault traces toward SW at the southern segment, while at the northern segment show almost straight fault traces. The emerging thrusts near the erosion surface have a high dip angle, ranging from (60°) to (85°) and the lateral length of these thrusts varied between (9.3 – 68 km). The southwestern limb of the structure was remained at subsurface from Ranya city to Bingrd district, this limb is related to thrust and strike slip faults and finally led to the development of Ranya Depression. The presence of numerous imbricate thrusts and its proximity to the Zagros Thrust Fault (ZTF) indicate that the Asos anticline is located within the IZ rather than the HFZ, as proposed by some other studies (e.g. <sup>(3, 13, 14)</sup>).

The AT1 affect the backlimb of the structure, and show the displacement estimated by (~100 m) which brought the Qamchuqa Formation over the Bekhme Formation. The AT2, AT3 and AT4 cut through the backlimb and surrounding area to the hinge zone, with the displacement is estimated by (360, 100 and 380 m) respectively on the surface and brought the Sarmord Formation over Qamchuqa formation. Whereas, AT4 interrupt the backlimb of the Anticline and override the older beds of Sarmord Formation on the younger layers of the same formation. The maximum dip- slip displacement occurred along the AT5 that cuts the NE forelimb of the structure, and displacement estimated by (~1000 m) on the surface. This led to transport the structure toward SW and brought the Early Jurassic Sarki Formation over the Early Cretaceous Sarmord Formation (Fig.2).

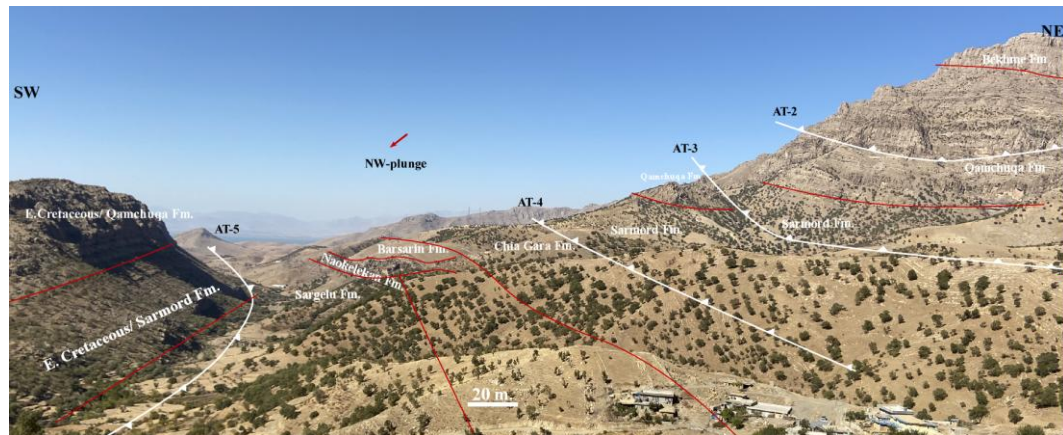


**Fig. 3: The field photo of Asos anticline as asymmetrical fold and Effect of thrusts at the core and both limbs of the Asos anticline.**

The Dokan (Dukan) anticlinal structure is also referred as Kosrat anticline in some previous studies<sup>(15, 16)</sup>. The age of the exposed sedimentary succession in this Anticline range from Early Cretaceous (Qamchuqa Fm.) to the Pleistocene (Bai-Hasan and Dokan Conglomerate) that represented by 15 formations.

The SW limb is slightly steeper and longer than the NE flank which makes the vergency of this anticline toward SW direction. The axial length of this fold is (~14 km) and the width is (~14.5 km), the crestal line of the Dokan anticline is about (982 m) and the maximum topography point at HSM reaches (1270 m). The hinge line is arcuate with the inner ward (hinterland) convex shape. The fold plunged southeasterly near Dokan Dam site that make an enechelon pattern with Surdash Anticline, while the northwestern plunge is interfered with Kosrat Anticline and dissected by a strike-slip fault (Fig. 4),<sup>(11)</sup> also indicated this fault as lineament that detected by gravity data. The anticline in the NE side separated from Qara Sard and Asos anticline by Joblagh and Ranya Synclines respectively (Fig. 2).

Four thrusts with opposite vergences and parallel to the anticline's hinge line disturbed the geometry of the Dokan structure. These thrusts are from NE to SW labeled as DT1, DT2, D3 and DT4 (Fig.2). The thrusts display either straight or very gently bowed traces towards hinterland in the map view.

Both DT1 and DT2 are backlimb thrusts that regarded as hinterland (NE) vergent thrust faults (back thrusts), while the remainders (DT3 and DT4) are forelimb thrust and interpreted as SW vergent listric thrust faults (Forethrusts) (Fig. 2 and Fig. 5). The backthrust DT-1 brought Dokan Conglomerate upward and the displacement reaches 95m, whereas, backthrust DKT-2 brought up Qamchuqa Formations on the surface and maximum dip-slip displacement on the fault at surface is (~300 m). The displacement on the forethrust DT3 is (~130 m), while the DT4 displaced more that 165m which led to Muqdadia Formation sitting on the Bai-Hasan Formation. The development of the pop-up structure can be attributed to the back thrust cutting up from the forethrust.

#### **4.2. Description and geometrical analysis of the Asos and Dokan anticline along cross section**

The Asos Anticline in the section has asymmetrical with steep SW forelimb and foreland vergency. While, the Dokan anticline's cross-sectional geometry reveals slightly an asymmetrical anticlinal structure with a SW foreland vergency and a steeply dipping axial surface toward NE. The SW forelimb of Asos anticline is shorter and steeper than its NE backlimb, while the SW limb of Dokan anticline is slightly steeper and longer than the NE limb.

The intelimb angle of Asos Anticline is (~113°) and has a box shape with wide hinge zone that displaced by the thrusts thrusting activity on the (e.g., AT2 fault ramp) which led to Qamchuqa and Bekhme Formations appear as prominent fault scarp along the back limb of the Asos Anticline, in contrast the intelimb angle of Dokan Anticline is

134° which have rounded, and broad box shape in the cross-section (Fig. 4 and Fig. 5). The anticlines have broad shape near the surface that becomes progressively narrower as it extends downward, while the nearby syncline exhibits the reverse opposite pattern. This fold architecture probably suggests parallel-fold style (Class 1B)<sup>(17)</sup>.



Fig. 4: A Field photo viewing the Dokan anticline. The Kometan Formation shapes the carapace of the Dokan anticline.

The cross-section reveals an amplitude of (2655 m) and an aspect ratio of 0.268 as calculated at the top of the Qamchuqa Formation at the Asos anticline. The cross-section of Dokan Anticline

shows an amplitude of (2627 m) and an aspect ratio of (0.199 %) as calculated of the same stratigraphic level which indicating a broad fold.

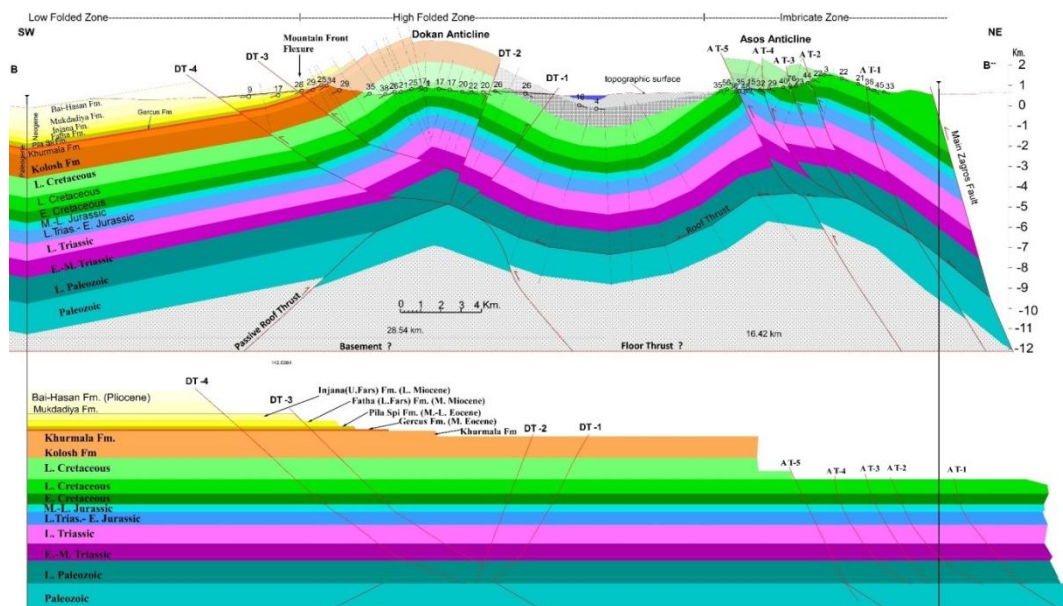


Fig. 5. Balanced and restored cross-section for the Asos and Dokan anticlines shown in cross-section A-A'.

#### 4.2.1. Geometrical analysis of the Asos and Dokan anticlines

In this study, the Asos and Dokan Anticlines analyzed geometrically along a traverse A-A' using stereographic projection and 235 bedding plane reading. The results from the synoptic

stereographic pi-diagram reveal that the SW limb of the Asos anticline has an average attitude of (213°/35°), while the NE limb is at (043°/32°) (Fig. 6). This indicates that the Asos Anticline has a slightly asymmetrical style. The interlimb angle is (113°), with the axial line plunged in (3°)

towards (128°), whereas the hinge surface is dipping toward (038°) and dips (88°), this means that the vergency is directed toward SW foreland. The Asos anticline classified as subhorizontal upright and open fold, according to (18).

The synoptic Pi- diagram [Figure \(6\)](#) displays the existence of two different aggregations of bedding poles clustered along the both flanks in the Asos Anticline. The presence of pole aggregations is a good indication that the structure is characterized by two dip domain at the limbs, one domain reflects steep dips and the other with gentle dip domain. one of them is steep dip panel and another has gentle dip domain. The propagation of the major thrusts led to an increase in the steepness of the dip panel and resulted in the rotation of the folded strata. The angular pattern of kink fold style often reflects the rotation and warping of beds

caused by fault ramp propagation. The existence of this style implies the presence of thrust-related anticlines, including thrust propagation anticline and thrust bend anticline (2, 19).

The synoptic stereographic pi-diagram of the Dokan anticline shows that the average attitude of the NE and SW limb are equal to (063°/21°) and (217°/25°) respectively, the orientation of hinge line (trend/ plunge) is (139°/5°), the attitude of axial surface is (049°/88°), and the interlimb angle equals to (135°) ([Fig. 6](#)). As a result, the Dokan Anticline structure has a slightly normal asymmetrical style with foreland vergency, and classified as a gentle fold. Similar to Asos anticline, the Dokan Anticline classified as subhorizontal upright fold according to the fold classification of (18).

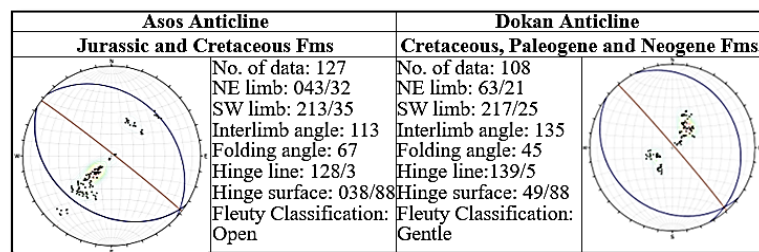


Fig. 6: Stereographic pi diagram of the Asos and Dokan anticlines and their geometrical elements.

#### 4.2.2. Estimation of the shortening amount in the Asos and Dokan anticlinal structures

In the structural cross-section, various types of shortening values have been estimated of the Asos and Dokan structures (space) at different stratigraphic levels (times). The fault-related shortening exhibits a general and gradual increase downdip in the cross-section ([Fig.5, table 1](#)). The down-section increase in fault displacement along the major thrusts causes the main reason of this cumulative vertical increase in thrust-related shortening value.

Unlike the fault-related shortenings, the fold-related shortening in the Asos anticlinal structure ranging between (2.17 km) and (3.239 km) and displays uneven and nonuniform changes in their

values upsection ([Fig. 5](#)), this irregular variation is mainly caused by irregular variations in wavelength to amplitude ratio and/or aspect ratio in different stratigraphic layers ([Fig. 5](#)). (20) concluded the same result of irregular variation in shortening value of Baradost Anticline in NW of Asos anticline. These results are coincident with other structural studies for instance, (21) clarified that the variations in fold amplitude and wavelength in the Rocky Mountain belt are influenced by the competent stratigraphic level. The partial shortening value from Early Cretaceous to Early Carboniferous which obtained after restoring the cross-section A-A<sup>-</sup> across Dokan anticline ranged between (2.52 (8.11 %)) and (2.02 (6.61 %)) with an average at (7.21%) (from Late Campanian to

Early Cretaceous) (Fig. 5, Table 1). Table (1) shows a general increase in shortening percentage down-section.

Similar to Asos anticline, the Dokan anticline revealed a gradual increase in thrust-related shortening down-section due to down-section increases in dip-slip displacement along major thrust faults. While, Fold-related shortening exhibits some non-uniform and slightly increase down-section which is results from changes in the fold amplitude and wavelength (Fig. 5, Table 1).

The horizontal shortening value accommodated by thrusts in the Asos Anticline is greater than their corresponding values in the Dokan Anticline structure (Table 1), because deformation intensity due to thrusting processes in the Asos Anticline (that located within the IZ) is greater than that in the Dokan Anticline (which is situated at HFZ).

The average horizontal shortening results that measured at top Qamchuqa Formation (Early Cretaceous) along cross-sections A-A<sup>-</sup> for the Asos and Dokan anticlines are (3.53 km) (17.70%) and (2.08 km) (6.79%), respectively (Table 1). The Average shortening percentage in the IZ, and HFZ of Asos and Dokan anticlines are measured at (17.05 %) and (7.21 %) respectively. The results of this research are consistent with previous studies

carried out in other areas of the ZFTB.<sup>(22)</sup> used the dip domain method and kinematically estimated shortening between (11 % – 15 %), (15.3 %) for Ranya Anticline (NW segment of Asos Anticline), (16.9 %) for Handren Anticline (adjacent to Asos Anticline), while for the Safeen and Bana Bawi Anticlines (within LFZ) measured at (14 %) and (4.5 %) respectively.

The value of shortening of Harir structure in HFZ (~24 km NW of Asos Anticline) ranging from (5.48 %) to (14.31 %) with an average (11.77 %) <sup>(23, 24)</sup>. calculated the shortening across Korek Anticline (which located at the NW plunge of Asos Anticline) that ranging between (7.83 %) and (20.31 %) and at top Qamchuqa Formation between measured at (15.07 %) <sup>(25)</sup>. yielded (14.19 %) in Bradost structure (IZ), (21.05 %) and (12.91 %) along Berat Anticline (HFZ). The Taq Taq Anticline (within LFZ) nearby the study area is shortened with an average of (6.67%) <sup>(26)</sup>. Shortening amount across the Duhok region along different section restoration varies from (7.13 %) to (19.71%) <sup>(27)</sup>. Others measured nearby shortening result in their studies around the study, for example: (11 %) <sup>(28)</sup>, (7.13 – 19.71 %) <sup>(29)</sup>, (15.3 %) and (20.7 %) in Cretaceous rocks (SE of the studied area) <sup>(30)</sup> and (22.7 %) <sup>(14)</sup>.

**Table 1. Calculation of shortening in different geological times within Asos and Dokan anticlinal folds.**

Top of Formation/age	Original Length (km)	Deformed Length (km)	Fault-related shortening (km)	Fold-related shortening (km)	Total Shortening (km)	Shortening (%)	Structure
Kometan/L. Campanian	18.98	16.09	0.604	2.286	2.89	15.23	Asos
Qamchuqa/E. Cretaceous	19.94	16.41	0.612	2.918	3.53	17.70	Asos
Sehkaian/E. Jurassic	19.51	16.41	0.787	2.313	3.10	15.89	Asos
Kurra chine/L. Triassic	19.61	16.41	0.915	2.285	3.20	16.32	Asos
Chia Zairi/Permian	19.92	16.41	1.1	2.410	3.51	17.62	Asos
Harur/E. Carboniferous	20.4	16.41	1.521	2.469	3.99	19.56	Asos
Pila Spi (M.-L. Eocene)	17.11	16.12	0.215	0.775	0.99	5.79	Dokan
Kometan/L. Campanian	30.61	28.54	0.441	1.629	2.07	6.76	Dokan
Qamchuqa/E. Cretaceous	30.62	28.54	0.457	1.623	2.08	6.79	Dokan
Sehkanian/E. Jurassic	30.76	28.54	0.611	1.609	2.22	7.22	Dokan
Kurra chine/L. Triassic	30.9	28.54	0.760	1.6	2.36	7.64	Dokan
Chia Zairi/Permian	31.06	28.54	1.051	1.459	2.51	8.11	Dokan
Harur/E. Carboniferous	31.07	28.54	1.06	1.46	2.52	8.14	Dokan
Average Shortening	Asos= 17.05%				Dokan= 7.21		

## 5. CONCLUSION

The studied structures are asymmetrical to slightly asymmetrical anticline with a steep forelimb. The average horizontal shortening value of the Dokan and Asos Anticlines is (7.21 %) and (17.05 %), respectively. The constructed cross-section reveals that the fault-related shortening generally decreases upsection across the Asos and Dokan structures, while the fold-related shortening at Asos Anticline shows non-uniform variation downward, but at Dokan Anticline increases downward. The Asos anticline exhibits greater fault-related shortening values compared to the Dokan structure, due to higher deformation intensity via thrusting processes in the Asos structure.

The geometry of balanced cross-section indicate that the development of the pop-up structure of Dokan Anticline can be attributed to the back thrust cutting up from the forethrust. The presence of numerous imbricate thrusts and its proximity to the ZTF or ZTF indicate that the Asos anticline is located in the ZIZ rather than the ZHFZ. Field investigations revealed that the Anah-Qaladiza

strike-faults caused segmentation of Asos Anticline.

**Conflict of interests:** The author declared no conflicting interests.

**Sources of funding:** This research did not receive any specific grant from funding agencies in the public, commercial, or not-for-profit sectors.

**Author contribution:** Author contributed in the study.

## Acknowledgments

We would like to extend our thanks to the Kurdistan Regional Government-Ministry of Natural Resources for their contribution of seismic sections and well data. Our gratitude goes to Dr. Hasan Balaki, Abdulla Othman, Barzan, Goran, Saman, Sherwan, and Burhan Hostani for their assistance during fieldwork.

## REFERENCES

- Poblet J, Lisle RJ. Kinematic evolution and structural styles of fold-and-thrust belts: The Geological Society of London London; 2011. <https://doi.org/10.1144/SP349.1>.

2. Suppe J, Medwedeff DA. Geometry and kinematics of fault-propagation folding. *Eclogae Geologicae Helvetiae*. 1990;83(3):409-54.
3. Jassim SZ, Goff JC. *Geology of Iraq: DOLIN*, sro, distributed by Geological Society of London; 2006.
4. Berberian M, King G. Towards a paleogeography and tectonic evolution of Iran. *Canadian journal of earth sciences*. 1981;18(2):210-65. <https://doi.org/10.1139/e81-019>
5. Al-Kadhimi JAM, Sissakian VK, Fattah AS, Deikran DB. *Tectonic map of Iraq, scale 1:1000 000, 2nd edition, Baghdad, Iraq: GEOSURV*. 1996.
6. Al-Qayim B, Omer A, Koyi H. Tectonostratigraphic overview of the Zagros suture zone, Kurdistan region, Northeast Iraq. *GeoArabia*. 2012;17(4):109-56. <https://doi.org/10.2113/geoarabia1704109>
7. Zebari M, Balling P, Grützner C, Navabpour P, Witte J, Ustaszewski K. Structural style of the NW Zagros Mountains and the role of basement thrusting for its Mountain Front Flexure, Kurdistan Region of Iraq. *J Structural Geology*. 2020;141:104206. <https://doi.org/10.1016/j.jsg.2020.104206>
8. Karim KH, Taha ZA. "ORIGIN OF CONGLOMERATIC LIMESTONE" DOKAN CONGLOMERATE" IN DOKAN AREA, KURDISTAN REGION, NE IRAQ. *Iraqi Bulletin of Geology Mining*. 2012;8(3):15-24. <https://ibgm-iq.org/ibgm/index.php/ibgm/article/view/203/197>
9. Woodward N, Boyer S, Suppe J. Balanced geological crosssections: an essential technique in geological research and exploration. *Short Course in Geology, Washington, DC. Am Geophys Union* 6:132p. 1989.
10. Mitra S. Balanced Structural Interpretations in Folds and Thrust Belts. *J Struct Geol*. 1992:53-77.
11. Qadir HO, Baban EN, Aziz BQ, Koyi HA. Potential field survey of subsurface structures of the NW segment of the Zagros Fold-Thrust Belt, Kurdistan Region. *Geophysical Prospecting*. 2023;71(8):1673-90. <https://doi.org/10.1111/1365-2478.13401>
12. Doski JA. Tectonic interpretation of the Raniya earthquake, Kurdistan, northern Iraq. *Journal of Seismology*. 2019;23(2):303-18. <https://doi.org/10.1007/s10950-018-9807-0>
13. Sissakian VK, Ghafur A, Omer H, Abdulhaq H. The Structural and Geomorphic Forms of Ranya Vicinity as Deduced from Satellite Images Data, Northeast Iraqi, Northeast Iraq. *The Iraqi Geological Journal*. 2022:172-85. <https://doi.org/10.46717/igj.55.2F.12ms-2022-12-27>
14. Le Garzic E, Vergés J, Sapin F, Saura E, Meresse F, Ringenbach J. Evolution of the NW Zagros Fold-and-Thrust Belt in Kurdistan Region of Iraq from balanced and restored crustal-scale sections and forward modeling. *Journal of Structural Geology*. 2019;124:51-69. <https://doi.org/10.1016/j.jsg.2019.04.006>
15. Al-Kubaisi MS, Barno JM. Fold geometry and kinematics of inversion tectonics for Kosrat anticline, northeastern Iraq. *Arabian Journal of Geosciences*. 2015;8:9469-80. <https://doi.org/10.1007/s12517-015-1864-x>
16. Ward AH, Al-Kubaisi MS. Geometry of Khalakan Anticline, Northeastern Iraq. *Tikrit Journal of Pure Science*. 2018;23(2):95-106. <http://dx.doi.org/10.25130/tjps.23.2018.034>
17. Ramsay JG. *Folding and fracturing of rocks*. McGraw-Hill book Co., New York.: Cambridge university press; 1967.
18. Fleuty M. The description of folds. *Proceedings of the Geologists' Association*. 1964;75(4):461-92. [https://doi.org/10.1016/S0016-7878\(64\)80023-7](https://doi.org/10.1016/S0016-7878(64)80023-7)
19. Suppe J. Geometry and kinematics of fault-bend folding. *American J science*. 1983;283(7):684-721.
20. Balaki HGK, Omar AA. Structural assessment of the Bradost and Berat structures in

Imbricate and High Folded zones—Iraqi Kurdistan Zagros belt. *Arabian Journal of Geosciences*. 2019;12(4):1-21. <https://doi.org/10.1007/s12517-019-4251-1>

21. McMechan M, editor 2012. Structural style and kinematic evolution of the Central Rocky Mountain foothills, British Columbia and Alberta. Canadian Society of Petroleum Geologists, GeoConvention 2012 Conference, Calgary-Canada; 2012.

22. Frehner M, Reif D, Grasemann B. Mechanical versus kinematical shortening reconstructions of the Zagros High Folded Zone (Kurdistan region of Iraq): *Tectonics*, 31. *TECTONICS*.2012;31(TC3002). <https://doi.org/10.1029/2011TC003010>

23. Omar A, Othman A. Morpho-structural study of the Korek Anticline, Zagros fold-thrust belt, Kurdistan of Iraq. *Geotectonics*. 2018;52(3):382-400. <https://doi.org/10.21271/ZJPAS.28.6.12>

24. Omar AA, Syan SH. Construction of a structural model for Harir anticline within Zagros Fold-Thrust belt, Kurdistan of Iraq. *ZANCO Journal of Pure and Applied Sciences*. 2017;28(6):90-105. <https://doi.org/10.1134/S0016852118030068>

25. Balaki HGK, Omar AA. Clues to inferred different thrust-related fold models and thin-thick skinned tectonics within a single folded structure in Iraqi Zagros, Kurdistan region. *Arabian Journal of*

*Geosciences*.2018;11(12):1-20.

<https://doi.org/10.1007/s12517-018-3605-4>

26. Syan SH, Omar AA. Structural Style of Taq Taq Anticline in the Zagros Fold-Thrust Belt in the Iraqi Kurdistan Region from the Integrated Surface and Subsurface Data. *The Iraqi Geological Journal*.2023;235-53.

<https://doi.org/10.46717/igi.56.2C.18ms-2023-9-24>

27. Doski JA, McClay K. Tectono-stratigraphic evolution, regional structure and fracture patterns of the Zagros fold-thrust belt in the Duhok region, Kurdistan, northern Iraq. *J Tectonophysics*.2022;838:229506.

<https://doi.org/10.1016/j.tecto.2022.229506>

28. Omar AA. An integrated structural and tectonic study of the Bina Bawi-Safin Bradost Region. Unpublished Ph D Thesis, Salahaddin University, Erbil. 2005:300p.

29. Al-Azzawi NK, Al-Khatony SE, Al-Sumaidaie MA. Detachment surface morphology and shortening distribution in the Foreland Folds of Iraq. *Iraqi National Journal of Earth Sciences*. 2014;14(1):39-58.

<https://doi.org/10.33899/earth.2014.87479>

30. Omar AA, Lawa FAA, Sulaiman SJAJoG. Tectonostratigraphic and structural imprints from balanced sections across the north-western Zagros fold-thrust belt, Kurdistan region, NE Iraq. *Arabian Journal of Geosciences*. 2015;8:8107-29.

<https://doi.org/10.1007/s12517-014-1682-6>